

## ISOTHERMAL OXIDATION BEHAVIOR OF PLASMA SPRAYED CONVENTIONAL AND NANOSTRUCTURED YSZ THERMAL BARRIER COATINGS

Alexandru PARASCHIV<sup>1</sup>, Alexandra BANU<sup>2</sup>, Cristian DOICIN<sup>2</sup>, Ion IONICA<sup>3</sup>

*In this study, conventional and nanostructured yttria-stabilized zirconia (YSZ) thermal barrier coatings (TBCs) were deposited by atmospheric plasma spraying (APS) on Ni superalloy with NiCrAlY as bond coat. The TBCs were exposed to isothermal oxidation tests in an electric furnace under air at 1100°C for 100, 200, 300, 400 and 600 hours and were investigated in terms of microstructure and microcomposition by using the scanning electron microscopy-energy dispersive X-ray spectroscopy (SEM-EDS). The nanostructured YSZ coatings showed a better performance at isothermal oxidation tests, in particular in terms of thickness of thermally grown oxide (TGO) layer which had a parabolic growth behavior.*

**Keywords:** TBCs, nanostructure, isothermal oxidation, TGO growth.

### 1. Introduction

The thermal barrier coatings (TBCs) are widely used to increase the turbine entry temperature (TET) and to protect from high temperature degradation of hot section in both aerospace and land-based turbine components. For more than four decades, yttria-stabilized zirconia has been used successfully as top coat in TBCs due to its outstanding material properties [1]. However, developing new TBCs or improving the actual TBCs to satisfy the multiple property requirements of a durable TBC has become a great challenge in the recent years [2].

A conventional TBC is composed of a NiCrAlY metallic bond coat and 7-8 wt.% yttria-stabilized zirconia (YSZ) ceramic top coat and is usually deposited by atmospheric plasma spraying (APS) or electron beam physical vapor deposition (EB-PVD). In the recent years, the nanostructured ceramic coatings have attracted many researches due to their promising properties, especially studies regarding the low thermal conductivity, bimodal microstructure and good mechanical properties [3].

<sup>1</sup> Eng., Romanian Research & Development Institute for Gas Turbines COMOTI, Romania, email: alexandru.paraschiv@comoti.ro

<sup>2</sup> Prof., Faculty of Industrial Engineering and Robotics, University POLITEHNICA of Bucharest, Romania

<sup>3</sup> Eng., Plasma Jet, Romania

During exposure at high temperature a thin and dense thermally growth oxides layer is formed at the interface between the metallic bond coat and ceramic coat. The increase of the thermally growth oxides (TGO) involves volumetric expansion in a constrained environment between top coat and bond coat which certainly results in the development of residual compression stresses [4] and when it reaches a critical value of 10-15  $\mu\text{m}$  will lead to degradation of TBCs system [5-7]. To evaluate the TGO growth and high temperature performance of TBCs isothermal oxidation tests are widely used in many studies.

A typical microstructural characteristic of the plasma-sprayed coatings TBC which has a great impact of their performances at high temperature is the porosity formed by micro- and nano-pores, microcracks, voids and discontinuities [8]. A higher level of porosity (more than 10%) of ceramic layer will improve the strain tolerance, sintering resistance and thermal insulation property of TBCs [9]. On the contrary, lower mechanical strength is obtained when the porosity is very high. Jamali et al. [8] shown that the size and morphology of microcracks and pores have a direct effect on adhesion and cohesion strength of TBCs. An image analysis technique based on SEM images was used in this work to measure the porosity.

The nanostructured and conventional YSZ were deposited by atmospheric plasma spraying on NiCrAlY bond coat with an Inconel 625 as substrate. The TBCs were tested under isothermal oxidation at 1100°C for holding time up to 600 hours. The isothermal oxidation behavior of nanostructured and conventional YSZ were comparatively studied in terms of microstructure and microcomposition evolution, porosity and TGO kinetics.

## 2. Materials and methods

In the present study the nickel-based superalloy plates (Inconel 625) with dimensions of 50 x 30 x 3 mm were used as substrate for atmospheric plasma spraying (APS) of TBCs. Before APS deposition of TBCs the Inconel 625 substrates were shot-blasted with alumina grit with sizes of 425-600  $\mu\text{m}$  under a pressure of 4 bars and then degreased with alcohol. For APS deposition of NiCrAlY bond coat commercial powders (Amperit 413 Sulzer Metco, USA) were used as feedstocks. Two commercial conventional (micrometric powders) and nanostructured (nanometric powders) 7-8%yttria - stabilized zirconia (YSZ) powders were used as feedstocks for APS deposition. The 8%  $\text{Y}_2\text{O}_3$  partially stabilized micro-sized zirconia powders (Metco 204NS-G, Sulzer Metco, USA) were used for APS deposition of conventional YSZ top coat. For APS deposition of nanostructured top coat 7%  $\text{Y}_2\text{O}_3$  partially stabilized nanostructured zirconia powders (Nanox Powder S4007, Inframet, SUA) were used. The morphology and microstructure of zirconia feedstock powders were examined using the scanning

electron microscope (SEM). The atmospheric plasma spraying of TBCs were deposited on Inconel 625 substrate by using a Sulzer-Metco F4-MB plasma gun (Sulzer-Metco, Switzerland) operated by a 6-axes robot (Kuka KR 150).

For atmospheric plasma spraying of both micrometric NiCrAlY and YSZ powders the process parameters provided from supplier powders were used (Table 1). Regarding the nanostructured YSZ powders, due to the higher average agglomerates size of nanostructured particles than conventional particles, a higher current (up to 530 A) and gas H<sub>2</sub> (up to 10.6 NLPM) were selected in order to increase the surface temperature and velocity of particles to achieve particle adhesion and cohesion on previous layers.

The process parameters used for atmospheric plasma spraying of TBCs investigated are presented in Table nr.1.

Table 1

Plasma spraying parameters for TBCs			
Parameters	NiCrAlY	YSZ conventional	YSZ nanostructured
Current, A	550	500	530
Voltage, V	67	68	60
Primary gas (Ar), NLPM	45	35	35
Secondary gas (H <sub>2</sub> ), NLPM	6	8	10.6
Powder feed rate, g/min	50	50	40
Spray speed, m/s	1.25	1.25	1.25
Spray distance, mm	120	120	125
Injector angle, °	90	90	90
Nozzle diameter, mm	6	6	8

The conventional and nanostructured YSZ coatings with a thickness of approx. 350 µm were plasma sprayed on NiCrAlY bond coat with a thickness of 150 µm. After APS deposition the specimens were prepared for experiments and investigations. For microstructural investigation and porosity measurements the samples with TBCs were metallographically prepared by using abrasive grinding papers ranging from very coarse (120 grit) to very fine (2500 grit) size and polishing on a felt pad diamond suspension of 3 µm and 1 µm.

## 2.1 Isothermal oxidation conditions

The conventional and nanostructured YSZ coatings were subjected of isothermal oxidation testing at 1100°C for holding duration of 100, 200, 300, 400 and 600 hours. Isothermal oxidation behavior of TBC systems were investigated using an electrical resistance furnace Nabertherm (Tmax=1400°C) with a heating rate of 15°C/min under isothermal oxidation conditions in an air atmosphere. After each oxidation cycle the furnace was cooled to ambient temperature and a specimen with conventional and nanostructured YSZ coatings were investigated.

## 2.2. Microstructural and microcompositional analysis

The microstructural and microcompositional analysis of the investigated TBCs were performed by using a scanning electron microscope FEI Inspect F50 equipped with an energy dispersive X-ray spectrometer EDAX (SEM - EDS). The effects of the high temperature oxidation on the investigated coatings were evaluated qualitatively by using the element distribution maps (EDS mapping) and quantitatively by using the local chemical composition analysis (EDS analysis).

## 2.3. Quantitative image analysis

To track the effects of the high temperature oxidation on the microstructure in terms of porosity the quantitative measurements of pores were performed using the image analysis software SCANDIUM (Olympus Soft Imaging Solutions GmbH). The evolution of the porosity was evaluated on the investigated TBCs by using SEM images at low magnification and targeting 12 areas. For a clearer assessment of the pores in the investigated samples, which can range from few hundred nanometers to several tens of microns, it was used the binarization technique of high resolution SEM images that associates the pixels with the pores and rest of material. The SEM images for the porosity evaluation were achieved by adjusting the brightness and contrast to highlight the pores. The images were subsequently converted into a 16-bit grayscale format followed by conversion into black and white threshold images. The microareas corresponding to the pores and the rest of the material were obtained by counting the pixels from the black and white regions.

## 3. Results and Discussions

### 3.1 Particle morphology and size distribution

Fig. 1a-c show the SEM images of NiCrAlY, conventional and nanostructured YSZ feedstock powders used in the thermal spray deposition. The NiCrAlY (Fig. 1a) and conventional YSZ (Fig. 1b) particles have a typical morphology of dense spray-dried particles, while the nanostructured YSZ particles (Fig. 1c) consist of agglomeration of YSZ nanoparticles into micron-sized spherical agglomerates. The mean particle sizes of NiCrAlY and powders were between 5-38  $\mu\text{m}$  while for the conventional and nanostructured YSZ were between 45-75  $\mu\text{m}$  and 15-150  $\mu\text{m}$ , respectively. Based on the smaller sizes of NiCrAlY and YSZ conventional particles it is expected that these particles will be fully molten or almost fully molten during plasma spraying.

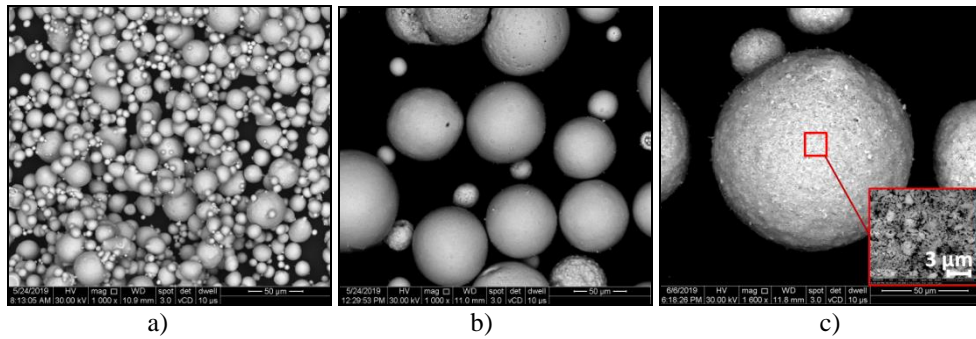


Fig. 1. SEM images of feedstock powders: (a) NiCrAlY powders for bond coat, (b) 7YSZ powders for conventional YSZ top coat and (c) 8YSZ agglomeration of nanoparticles for nanostructured YSZ top coat

### 3.2 Microstructure and microcomposition of as-sprayed coatings

Cross-sectional images and outer surface morphology of the conventional and nanostructured YSZ coatings were obtained by using SEM (Fig. 2-3).

Fig. 2a-c show the microstructure of as-sprayed TBC with conventional YSZ as top coat (Fig. 2a-b) and its chemical composition based on its energy-dispersive X-ray spectroscopy (EDS) spectrum (Fig. 2c). As can be observed in Fig. 2a-b the microstructure of as-sprayed TBC with conventional YSZ as top coat has typical characteristics of a thermal spraying by APS technique and consists of micrometer-sized lamellar grain structures of zirconia with microcracks, globular and intersplat pores on both metallic and ceramic coating structure.

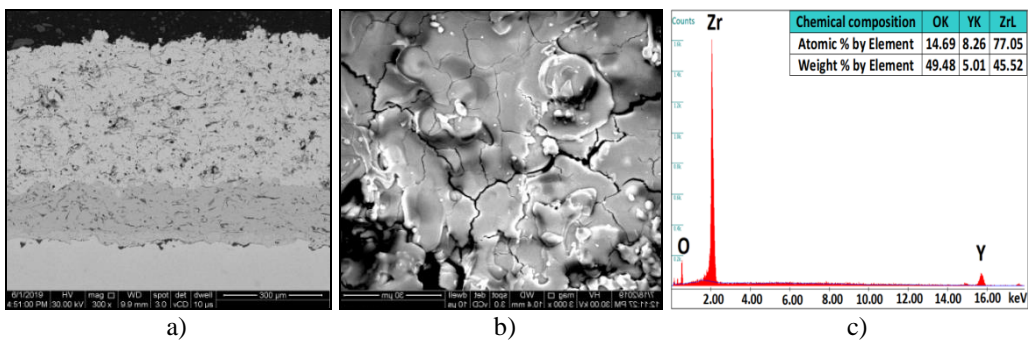


Fig. 2. The SEM-EDS images of the conventional YSZ coating: (a) cross section; (b) outer surface morphology; (c) energy-dispersive X-ray spectroscopy (EDS) spectrum and global chemical composition of conventional YSZ coating

Fig. 3a-c show the microstructure of as-sprayed TBC with nanostructured YSZ as top coat (Fig. 3a-b) and the global chemical composition based on its energy-dispersive X-ray spectroscopy (EDS) spectrum (Fig. 3c). The SEM investigation highlighted that the nanostructured zirconia coatings mainly

contained a bimodal microstructure consisting of micrometer-sized lamellar grain structures of zirconia with splats, pores and microcracks, similar to those of conventional YSZ (Fig. 2a-b) and nanosized zirconia particles which are also called “nanozones” embedded in the matrix (detail from Fig. 3b). The nanozones with fine grains with size ranging from 30 to 100 nm (Fig. 3b) result from non-molten or partially molten of nanostructured agglomerated YSZ particles in the plasma jet while the lamellar splats are the result of flattening of fully molten particles.

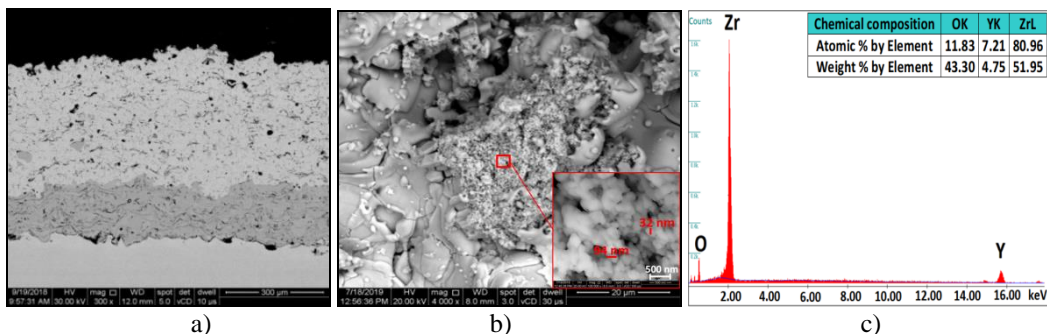


Fig. 3. The SEM-EDS images of the nanostructured YSZ coating: (a) cross section; (b) outer surface morphology; (c) energy-dispersive X-ray spectroscopy (EDS) spectrum and global chemical composition of nanostructured YSZ coating

### 3.3 Porosity

Usually, in plasma-sprayed coatings the porosities are attributed to the insufficient local plastic deformation of the particles after impacting with the previous splats. Generally, in conventional TBCs deposited by APS technique there are two categories of pores: coarser pores with dimensions between a few microns and tens of microns and finer pores with dimension of hundred nanometers. The coarser pores appear as a result of incomplete melting of the pulverized particles which generate interstices during flattening of splats. Also, the intra- and inter-lamellar microcracks which appeared during thermal deposition are also associated with the coarser pores. Regarding the finer pores they are generated by the incomplete contact between splats.

In the case of nanostructured YSZ coating a third type of porosity is associated with the nanozones (detail from Fig. 3b). The trimodal distribution of pores usually have a positive impact during exposure at high temperature of TBCs by increasing the durability at thermal shock [10] and decreasing the thermal diffusivity and elastic modulus of TBCs [2].

The pores and their evolution during isothermal oxidation were identified by thresholding the brightness of the pores to produce binary images and determining the percentage of the dark area fraction. In the as-sprayed state, the

conventional YSZ had a higher porosity of 16.2% than nanostructured coating of 10.9%. Beside the different APS parameters, the higher level of microcracks had a great influence on the higher porosity of YSZ conventional. Fig. 4 shows the average and standard deviation porosity values for nanostructured and conventional YSZ coatings in the as-sprayed state and isothermal oxidation durations of 100, 200, 300 and 600h at 1100°C.

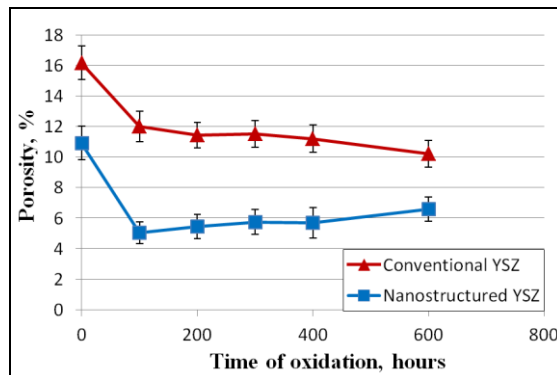


Fig. 4. The evolution of porosity in YSZ conventional and YSZ nanostructured as a function of holding durations of 100, 200, 300, 400 and 600 hours at 1100°C

The difference between the levels of porosity from the investigated coatings was preserved during the oxidation durations. During isothermal oxidation testing, both YSZ coatings present a reduction of porosity of more than 60% as a result of densification of ceramic layer. The densification is generated by the sintering process which occurred in zirconia layer during exposure at high temperatures [11]. The sintering process has negative effects in TBC coatings by increasing the thermal conductivity and elastic modulus and losing the strain tolerant behavior [11]. The porosity in conventional coatings decreased in the first 200 hours (from 16.2% to 11.4%) and then had a slight and constant decrease to 10.2% after 600 hours of isothermal oxidation. This is a typical behavior for conventional coatings where the porosity decreases with increasing temperature and holding duration of oxidations [12].

A similar trend was observed in the case of nanostructured YSZ in the first 100 hours when the porosity had a significantly decreased from 10.9 to 5%. But, after this stage, the porosity had a slight and constant increasing trend up to 6.6% after 600 hours of isothermal oxidation. This behavior can be explained with the bimodal microstructure of YSZ nanostructured coating made of nano- and micro-structured zones. There are many studies [2,3,11] that highlight the reducing effect of the sintering process by using nanostructured coatings. During isothermal oxidation testing the nanozones may experience significantly higher shrinkage than remolten splats due to the intrinsic tendency of nanosized structures towards densification and will open the pores and increase the size of

discontinuities between the nano- and micro-structured zones [12]. In addition, a high pressure must be exerted to allow agglomerated nanoparticles to be rearrangement, in order to attain high densities during oxidation. In this way, the effects of sintering process to reduce the porosity and its benefits are inhibited by the microstructural characteristics of the YSZ nanostructured which act as a barrier to impede sintering.

### 3.4 Thermally grown oxide

During exposure at high temperature for different time periods, the TGO layer is formed at the interface between bond coat and ceramic top coat as a result of penetration of oxygen from ceramic coat and interaction with the aluminium in the metallic layer. Microstructural investigations on the isothermal oxidation behavior and TGO formation at each time of oxidation were performed. The TGO thicknesses of the investigated TBCs at each oxidation cycle were also measured by quantitative SEM image analysis. The average TGO thickness was calculated based on 60 measurements from 12 SEM images obtained at x1200 magnification for each specimen. In Fig. 5a-b are presented the SEM images of the evolution of microstructure and thickness of TGO layer during exposure at 1100°C for exposure times of 100, 200, 300, 400 and 600 hours for both conventional (Fig. 5a) and nanostructured YSZ coatings (Fig 5b).

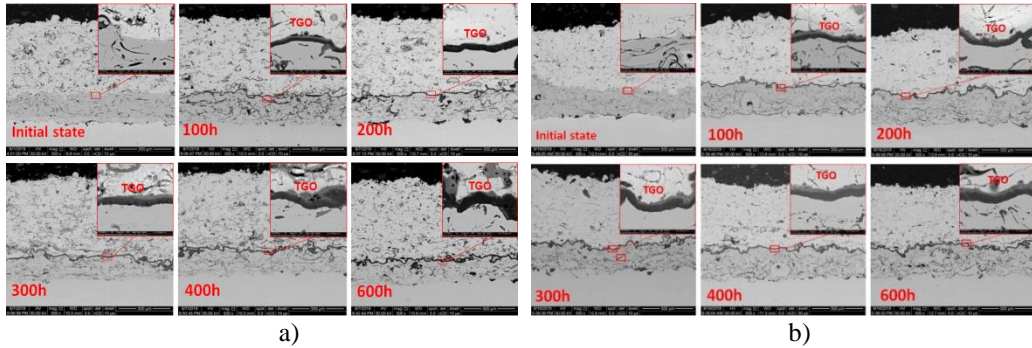


Fig. 5. The cross-sectional SEM images of the evolution of thickness of TGO layer during exposure at 1100°C for exposure times of 100, 200, 300, 400 and 600 hours: (a) conventional YSZ; (b) nanostructured YSZ

After the oxidation tests, even after holding time of 600 hours, no defects such as spallation, chipping or major cracks were observed. During thermal exposure in air, oxidation of the metallic bond coat produced along the bond coat/top coat interface an irregular TGO layer. At the first stage of oxidation the TGO layer consists of a high content of aluminium and oxygen elements which form the  $\alpha$ - $\text{Al}_2\text{O}_3$ . At the first stage (the first 100h) of oxidation  $\text{Al}_2\text{O}_3$  form (dark gray) does not undergo a structural change and exhibits a dense structure while

the mixed oxide structures (light gray) was observed outside the  $\text{Al}_2\text{O}_3$  oxide layer in a time-dependent manner. The initial fast growth of TGO is attributed to the availability of aluminium from the Al-rich  $\beta$ -phase and formation of  $\text{Al}_2\text{O}_3$  and firstly depends on the diffusion of atmospheric oxygen through the ceramic porous [14]. During extended thermal exposure some oxide clusters of chromia ( $\text{Cr}_2\text{O}_3$ ), spinel oxides which are a mixture of  $\text{NiCr}_2\text{O}_4$ ,  $\text{NiAl}_2\text{O}_4$ ,  $\text{CoAl}_2\text{O}_4$ ,  $\text{CoCr}_2\text{O}_4$ ,  $\text{NiCo}_2\text{O}_4$  or small amount of  $\text{CoO}$  and  $\text{NiO}$  may be formed in TGO near ceramic coat [14]. The formation of these oxides is attributed to the localized low aluminium concentration in bond coat near top coat/bond coat interface. The amount of oxides increases with increasing the isothermal oxidation time and some  $\text{Al}_2\text{O}_3$  and  $\text{Cr}_2\text{O}_3$  spread more in NiCrAlY coating of conventional than nanostructured TBCs when the oxidation time was more than 300h.

Due to the open pores and microcracks the conventional YSZ coating ensures an easier penetration of oxygen to the bond coat. In addition, the increased isothermal oxidation resistance may be also related to the grain refining of the nanostructured zirconia coating. The oxidation behavior of TBC revealed that TGO layer growth is predominantly controlled by the element diffusion. The chemical composition identified by EDS and X-ray maps showed that the inner layer of TGO is composed of  $\text{Al}_2\text{O}_3$  and outer is composed of a mixture of oxides with a high amount of Ni and Cr (Fig. 6).

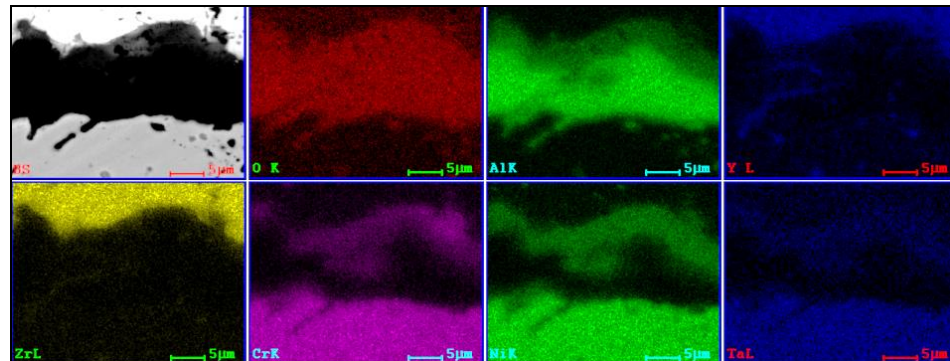


Fig. 6. EDS elemental maps of inner and outer layers of the TGO at the NiCrAlY/conventional YSZ interface after 600 hours of oxidation

During the tests a time-dependent increase in the thickness of TGO layer was observed. The variations of TGO thickness as a function of oxidation time were plotted in Fig. 7 for each type of TBC. All measurements were made on the regions where TGO layer was continuous, while regions with non-uniform TGO layer were excluded.

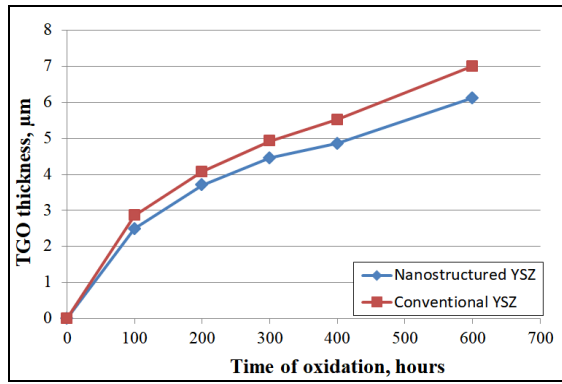


Fig. 7. The growth of TGO layer versus time of oxidation at 1100°C for conventional and nanostructured TBCs

Fig. 7. shows an increase in the thickness of TGO layer after 100, 200, 300, 400 and 600 hours of oxidation at 1100°C for both conventional and nanostructured YSZ. The average TGO thickness had a parabolic growth behavior as a function of oxidation time for both conventional and nanostructured YSZ coatings. The parabolic growth behavior of TGO is typical for oxidized TBCs at high temperature [5,6,14,15]. Generally, the growth of TGO in conventional YSZ is higher than nanostructured YSZ [2, 3, 6]. After exposure times of 100 hours of oxidation the average thickness of TGO layer for conventional and nanostructured YSZ was  $2.6 \pm 0.2$  µm and  $2.3 \pm 0.5$  µm, respectively, while the maximum TGO thickness was  $7 \pm 1.6$  µm and  $6.1 \pm 1.4$  µm, respectively, after exposure times of 600 hours of oxidation. The TGO layer in the two kinds of TBCs growth followed parabolic laws and the rate of oxidation can be expressed as the TGO thickness ( $d_{TGO}$ ) or as the mass gain rate ( $W/A$ )<sup>2</sup> [14,15] by using the following equation,

$$d_{TGO} = k_p (t_{T_{max}})^n \quad (1)$$

where,  $d_{TGO}$  is the thickness of the TGO layer or the mass gain per unit area ( $W/A$ )<sup>2</sup>,  $k_p$  is the oxidation coefficient (the parabolic rate constant for oxidation),  $t_{T_{max}}$  is the exposure time at maximum temperature and  $n$  is the oxidation exponent [5]. It was found that by using  $n=2.5$  a good fit at experimental data at 1150 and 1050°C can be used to describe the kinetics of TGO formation in TBCs [16]. For the conventional and nanostructured YSZ TBCs oxidized at 1100°C the  $k_p$  was  $1.977 \times 10^{-17}$  m<sup>2</sup>/s (0.2668 µm/h<sup>0.5</sup>) and  $1.6362 \times 10^{-17}$  m<sup>2</sup>/s (0.2427 µm/h<sup>0.5</sup>), respectively. These values are slightly lower than those obtained by Jackson et al. [16] for conventional TBCs, which were between  $1.05 \times 10^{-17}$  m<sup>2</sup>/s at 1050°C and  $5.84 \times 10^{-17}$  m<sup>2</sup>/s at 1150°C. A. Keyvani et al. [5] obtained an oxidation resistance for the conventional and nanostructured YSZ exposed at 1100°C of  $d_{TGO} = 0.5107 (t_{T_{max}})^{0.4218}$  ( $k_p$  is approx. 0.5 µm/h<sup>0.4</sup>) and  $d_{TGO} = 0.4217$

$(t_{T_{max}})^{0.4190}$  ( $k_p$  is approx.  $0.4 \mu\text{m}/\text{h}^{0.4}$ ), respectively. These differences between the calculated values of  $k_p$  are mainly caused by the characteristics of the TBCs, oxidation test conditions and calculation methods.

The superior isothermal oxidation resistance of nanostructured versus conventional YSZ was also observed in other works [2, 3, 6]. A. Keyvani et al. [6] indicated in their study the feasibility of using the nanostructured YSZ in order to improve the performances of TBCs at high temperatures. This behavior significant increases the durability and performances of TBC system in the service condition of gas turbines and is mainly attributed to less oxygen diffusion through the nanozones, pores and fine grained of nanostructured YSZ than in the compacted conventional YSZ.

## 6. Conclusions

Based on the experimental results it can be concluded that both conventional and nanostructured YSZ coatings deposited by APS technique had long spallation lifetime of at least 600 hours at  $1100^\circ\text{C}$ , without causing spallation chipping, major crack or any degradation which promising a good isothermal oxidation resistance.

During isothermal oxidation, the porosity decreased of more than 60% due sintering effects in both YSZ coatings.

The average of TGO thickness had a parabolic growth behavior as a function of holding time for both conventional and nanostructured YSZ TBCs. The amount of oxides  $\text{Al}_2\text{O}_3$  and some oxide clusters of chromia and spinel oxides spread more in NiCrAlY coating of conventional than nanostructured TBCs when the oxidation time was longer than 300 hours.

The rate of oxidation  $k_p$  was  $1.977 \times 10^{-17} \text{ m}^2/\text{s}$  ( $0.2668 \mu\text{m}/\text{h}^{0.5}$ ) for conventional YSZ TBCs and  $1.6362 \times 10^{-17} \text{ m}^2/\text{s}$  ( $0.2427 \mu\text{m}/\text{h}^{0.5}$ ), respectively. This indicate a superior isothermal oxidation resistance of the nanostructured compared to conventional YSZ which can be attributed to less oxygen diffusion through the nanozones, pores and fine grained of nanostructured YSZ than in the compacted conventional YSZ.

## Acknowledgements:

This work was carried out within POC-A1-A1.2.3-G-2015, ID/SMIS code: P\_40\_422/105884, "TRANSCUMAT" Project, Grant no. 114/09.09.2016 (Subsidiary Contract no. 5/D.1.3/114/18.12.2017), Project supported by the Romanian Minister of Research and Innovation.

## R E F E R E N C E S

- [1]. *R. A. Miller*, “Thermal barrier coatings for aircraft engines: history and directions”, *J. Therm. Spray Technol.* vol.**6**, no.1, (1997), pp. 35–42
- [2]. *R. S. Lima, B. R. Marple*, “Nanostructured YSZ thermal barrier coatings engineered to counteract sintering effects”, *Materials Science and Engineering A* **485**, (2008), pp. 182–193
- [3]. *J. Sun, L. Zhang, D. Zhao*, “Microstructure and thermal cycling behavior of nanostructured yttria partially stabilized zirconia (YSZ) thermal barrier coatings”, *Journal of Rare Earths*, Vol. **28**, Spec. Issue, Dec. 2010, pp. 198
- [4]. *H. Dong, G.-J. Yang, C.-X. Li, X.-T. Luo, and C.-Ji. Li*, “Effect of TGO Thickness on Thermal Cyclic Lifetime and Failure Mode of Plasma-Sprayed TBCs”, *J. Am. Ceram. Soc.*, **97**, (2014), pp.1226–1232
- [5]. *A. Keyvani, M. Saremi, M. H. Sohi, Z. Valefi*, “A comparison on thermomechanical properties of plasma-sprayed conventional and nanostructured YSZ TBC coatings in thermal cycling”, *Journal of Alloys and Compounds* **541**, (2012), pp.488–494
- [6]. *A. Keyvani, M. Saremi, M. H. Sohi*, “Oxidation resistance of the nanostructured YSZ coating on the IN-738 superalloy”, *Journal of Ultrafine Grained and Nanostructured Materials*, vol.**47**, No.2, Dec 2014, pp.89-96
- [7]. *H. Jamali, Mozafarinia, R. Razavi, R. Ahmadi-Pidani, M. Reza Loghman-Estarki, M.* Fabrication and Evaluation of Plasma-Sprayed Nanostructured and Conventional YSZ Thermal Barrier Coatings”, *Curr. Nanosci.* **8**, (2012), pp.402–409
- [8]. *J. G. Odhiambo, W. Li, Y. Zhao, and C. Li*, “Porosity and Its Significance in Plasma-Sprayed Coatings Coatings“, vol. **9**, no. 460 (2019), pp.1-19
- [9]. *G. D. Girolamo, A. Brentari, and E. Serra*, “Some recent findings on the use of SEM-EDS in microstructural characterisation of as-sprayed and thermally aged porous coatings: a short review“, *AIMS Materials Science*, vol.**3** no.2, (2016), pp. 404-424
- [10]. *A. Scrivani, G. Rizzi, U. Bardi, C. Giolli, M. Muniz Miranda, S. Ciattini, A. Fossati, and F. Borgioli*, “Thermal Fatigue Behavior of Thick and Porous Thermal Barrier Coatings Systems”, *JTTEE5*, **16**(5-6), (2007), pp. 816–821
- [11]. *A. Portinha, V. Teixeira, J. Carneiroa, J. Martinsb, M.F. Costac, R. Vassend, D. Stoever* “Characterization of thermal barrier coatings with a gradient in porosity”, *Surface & Coatings Technology* **195**, (2005), pp. 245– 251
- [12]. *L. Baiamonte, F. Marra, G. Pulci, J. Tirillò, F. Sarasini, C. Bartuli, T. Valente*, “High temperature mechanical characterization of plasma-sprayed zirconia–yttria from conventional and nanostructured powders, *Surface & Coatings Technology* **277**, (2015), pp. 289–298
- [13]. *X. Liu, T. Wang, C. Li, Z. Zheng, Q. Li*, “Microstructural evolution and growth kinetics of thermally grown oxides in plasma sprayed thermal barrier coatings “, *Progress in Natural Science: Materials International* **26**, (2016), pp. 103–111
- [14]. *E. M. Anghel, M. Marcu, A. Banu, I. Atkinson, A. Paraschiv, S. Petrescu*, Microstructure and oxidation resistance of a NiCrAlY/Al<sub>2</sub>O<sub>3</sub>-sprayed coating on Ti-19Al-10Nb-Valloy”, *Ceramics International* **42**, (2016), pp. 12148–12155
- [15]. *A. Banu, M. Marcu, S. Petrescu, N. Ionescu, and A. Paraschiv*, ”Effect of niobium alloying level on the oxidation behavior of titanium aluminides at 850°C”, *International Journal of Minerals, Metallurgy and Materials* vol. **23**, No. 12, December 2016, pp. 1452-1257
- [16]. *R. D. Jackson, M. P. Taylor, H. E. Evans, Xin-Hai Li*, “Oxidation Study of an EB-PVD MCrAlY Thermal Barrier Coating System”, *Oxid Met* **76**, (2011), pp. 259–271.